Pergamon

*Phys. Chem. Earth (B)*, Vol. 25, No. 4, pp. 381–385, 2000

1464-1909/00/$ - see front matter

PII: S1464-1909(00)00030-7

# Pore-Water Pressure of Debris Flows

**Norifumi Hotta and Takehiko Ohta**
Graduate School of Agricultural and Life Sciences, The University of Tokyo, Japan

*Received 23 April 1999; Revised; 3 November 1999; accepted 25 January 2000*

**Abstract.** Until now, the pore water pressure, which is one of the stress constituents governing the flow characteristics of a steady, laminar debris flow, has been considered to be hydrostatic. We succeeded in measuring the pore water pressure distribution in solid-water phase flows with a rolling mill. The experimental results show that the pore water pressure actually exceeds the hydrostatic pressure, and indicates that the excess pore water pressure arises as a consequence of Reynolds stresses due to the shearing of interstitial water.


## 1 Introduction.

In mountainous regions of Japan, debris flows often cause human and environmental disasters. Therefore, much research on debris flows has been conducted. Some of the current models of debris flows are based on Bagnold's work (1954), but these models vary in their treatment of stress structure, which is considered to govern the nature of the flows. It has been difficult to confirm the values of the individual internal stresses in debris flows experimentally, largely because of the difficulty in making direct measurements in an open channel. Here, we present the pore water pressure distribution of a solid water phase flow, measured in a rolling mill. Our findings indicate that the pore water pressure of debris flows exceeds the hydrostatic pressure.

## 2 Constitutive equations of debris flows.

### 2-1 Constitutive equations.

From a dynamic viewpoint, debris flows can be roughly classified as laminar or turbulent flows. A laminar debris flow is here defined as a flow in which the average streamlines of gravel particles are parallel (Itoh and Egashira, 1999) while when groups of gravel pieces are irregularly mixed downstream by the current, the debris flow is defined turbulent (**Fig.1.**). However, the interstitial water of a laminar debris flow is in turbulent condition because it is strongly sheared by particles.

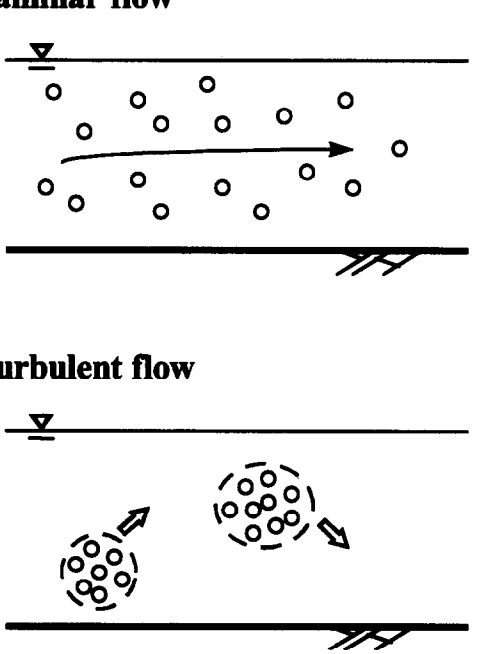


**Fig.1.** Concepts of laminar and turbulent debris flow

As Itoh and Egashira (1999) pointed out, some laminar flow studies have been conducted that primarily focus on constitutive equations. For a steady, uniform debris flow (**Fig.2.**), momentum conservation equations lead to the following relationships for the isotropic total pressure, $p$, and the total shear stress, $\tau$:

$$p = \int_y^h \{(\sigma - \rho)c + \rho\} g \cos\theta dy \quad (1)$$

*Correspondence to*: Norifumi Hotta

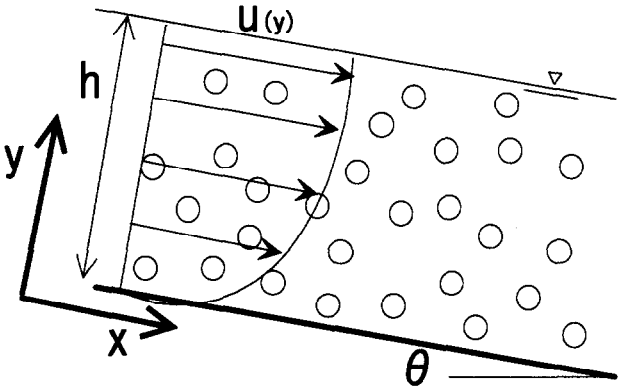


**Fig.2.** Sketch of a steady, uniform debris flow

$$\tau = \int_y^h \{(\sigma - \rho)c + \rho\} g \sin\theta dy \tag{2}$$

in which $h$ is the flow depth, $g$ is the acceleration due to gravity, $\theta$ is the bottom inclination with respect to the horizontal plane, $\sigma$ is the mass density of sediment particles, $\rho$ is the mass density of water, and $c$ is the volumetric concentration of sediment. In theoretical discussions, Egashira, *et al.* (1989; 1992, 1997) and Miyamoto (1985) proposed the following expressions for $p$ and $\tau$:

$$p = p_s + p_d + p_w \tag{3}$$

$$\tau = \tau_y + \tau_d + \tau_f \tag{4}$$

in which $p_s$ is the pressure due to static contact between particles, $p_d$ is the dynamic pressure due to inelastic particle-to-particle collisions, $p_w$ is the hydrostatic pressure of interstitial water, $\tau_y$ is the yield shear stress, $\tau_d$ is the shear stress due to inelastic particle-to-particle collisions, and $\tau_f$ is the Reynolds shear stress due to the shearing of interstitial water.

Since $\tau_y > \tau_d + \tau_f$ (and $p_s > p_d + p_f$) in debris flows treated in this study (i.e. steady, uniform and laminar debris flows), it is important to consider $\tau_y$ in researching the stress structure of debris flows. Egashira *et al.* (1997) studied $p_s$ and $\tau_y$. However, it is also important to estimate $\tau_d$ and $\tau_f$ to investigate the fluid characteristics of debris flows, since they are included in the functions of *du/dy*. Miyamoto (1985) confirmed that the theoretical value of $\tau_d$ corresponded with experimental estimates, but could not confirm the value for $\tau_f$ mainly because of technical difficulties.

## 2-2 Pore-water pressure.

It is usually assumed that the pore water pressure, $p_w$, in Eq. (3) is hydrostatic, but the presence of $\tau_f$ assures us that there is excess pore water pressure, $p_f$, as Reynolds stress. Therefore, the pore water pressure of debris flows must not be hydrostatic, and is expressed as

$$p_w = p_h + p_f \tag{5}$$

in which $p_h$ is the hydrostatic pressure of debris flows ($= \rho g(h-y)$). If the fluctuating component of velocity is isotropic, the following equation is obtained:

$$\tau_f = \rho\overline{u'v'} \approx \rho\overline{u'u'} = p_f \tag{6}$$

in which $u'$ and $v'$ are fluctuating velocity components of interstitial water in the x and y directions, and $\rho\overline{u'v'}$ and $\rho\overline{u'u'}$ are Reynolds stresses. Eq. (6) shows that information about $\tau_f$ can be obtained by measuring $p_f$, the excess pore water pressure. Furthermore, according to Prandtl's mixing length theory

$$p_f = \rho\overline{u'u'} = \rho l^2 \left(\frac{d\overline{u}}{dy}\right)^2 \tag{7}$$

in which $l$ is the mixing length and $\overline{u}$ is the mean velocity of the interstitial water.

The velocity of interstitial water, $U$, can now be expressed as

$$U = \overline{u} + u' \tag{8}$$

In this study, we focus our attention on debris flows of laminar type defined previously. In particular, here we assume that the average velocity of the debris flow $u$ is equal to the average water velocity $\overline{u}$.

The mixing length in Eq. (7) is related to the scales of the interstices between particles. Egashira *et al.* (1989) proposed the following expression for $l$:

$$l = k_f \left(\frac{1-c}{c}\right)^{\frac{1}{3}} d \tag{9}$$

in which $d$ is the sediment particle size and $k_f$ is an empirical constant specified as $k_f \cong 0.25$. On the other hand, the typical velocity distribution in a laminar debris flow moving over a rigid bed is given:

$$u = \frac{5}{3} u_m \left\{1 - \left(1 - \frac{y}{h}\right)^{3/2}\right\} \tag{10}$$

in which $u_m$ is the mean channel velocity. Note that this velocity profile has been found to agree satisfactorily with experimental debris flow velocity distribution (e.g. Egashira, *et al.*, 1989; Takahashi, 1980). Then substitution Eq. (9) and Eq. (10) into Eq. (7) yields:

$$p_f = {k_f}^2 \left(\frac{1-c}{c}\right)^{\frac{2}{3}} \rho \frac{25{u_m}^2}{4h^2} d^2 \left(1 - \frac{y}{h}\right) \tag{11}$$

that is the distribution of $p_f$ along the flow depth. If the sediment particles are uniformly distributed in the y direction, $p_f$ increases linearly from the surface to the bed.

## 3 Measuring $p_f$.

3-1 Experimental Setup.

Experiments aimed at measuring the pore-water pressure of solid water phase flows in open channels. However, these experiments encountered difficulties in maintaining a prolonged steady flow.

To avoid this problem, we used a rolling mill similar to those used in abrasion experiments (e.g. Krumbein, 1941; Kuenen, 1956). The experimental setup is shown in **Fig.3**. A cylinder 20cm in diameter and 4cm deep made of acrylic resin was connected to a motor, and 4mm glass beads were glued inside the cylinder to simulate bed roughness.

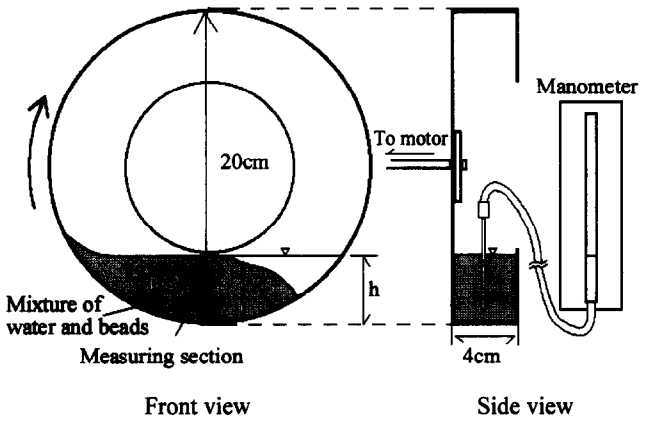


**Fig.3.** Sketch of the experimental setup

Hotta *et al.* (1998) examined factors other than Reynolds stress that may also cause excess pore water pressure in experiments with a rolling mill, such as centrifugal force and infiltration flows. Their results allowed us to conclude that these other factors play a minor role in this study.

3-2 Experimental Arrangement.

Glass and plastic beads 6mm in diameter with respective specific gravities of 2.6 and 1.3, were mixed with water in a ratio of 50 $cm^3$ beads per 130 $cm^3$ water. While the rolling mill containing the mixture was rotating steadily, the velocity profile of the mixtures was measured analyzing the trajectories of particles filmed through video camera, to verify Eq. (10).

The mean concentrations of the granular flow $c_*$ were also roughly estimated analyzing the recorded images. Whereas the sediment concentration in the mixture was 0.28 according to the 5:13 mixing ratio, the actual mean concentration of the granular flow exceeded 0.28, because the granular flow phase (A) and water phase (B) were separated in front of the flow as shown in **Fig.4**. Measuring the area of the two zones A and B allowed to estimate the mean concentration of the granular flow phase $c_*$ from the following equations:

$$c_* \cdot A_w = A_p \tag{12}$$

$$A_p + A_w = A \cdot W \tag{13}$$

$$A_p = {}^{5}\!/_{13}(A_w + B \cdot W) \tag{14}$$

in which $A_w$ is the water volume and $A_p$ is the particle volume in the granular flow, $A$ is the area of the granular flow phase, $B$ is the area of the water phase, and $W$ is the width of the rolling mill, which is equal to 4cm. Assuming as a first approximation that the beads are distributed uniformly within the mixture, the values of $c_*$ yields an estimate of the volumetric particle concentration $c$.

Finally, the excess pore water pressure distribution was measured in the y direction using a pitot tube with an internal diameter of 1mm.

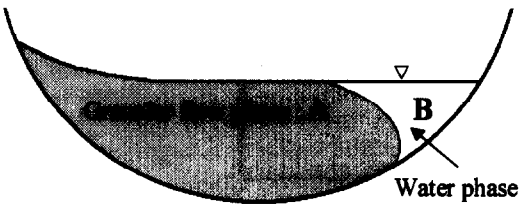


**Fig.4.** Granular flow in the rolling mill

## 4 Discussion of the results.

**Figure 5** shows the velocity profiles in the rolling mill. The velocity profiles are plotted setting the velocity at the bottom of the rolling mill as zero. The velocity profiles of both glass bead mixtures and plastic bead mixtures agree satisfactorily with the velocity profile described by Eq. (10). This suggests that a strict similarity exists between the dynamic conditions within the rolling mill and uniform debris flow in open channels, thus supporting the use of Eq. (11).

The relationship between the mean sediment

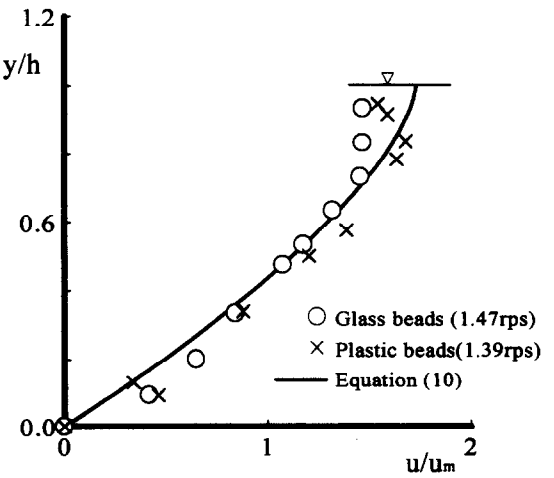


**Fig.5.** The velocity profiles measured in the measuring section of the rolling mill are compared with the theoretical velocity profile given by eq. (10).

concentration $c_*$ and the rotation speed $\omega$ (revolution/sec.: rps) of the rolling mill is shown in **Fig.6**. The maximum and minimum mean concentrations estimated for the glass and plastic bead mixtures are nearly equal, the concentration of glass beads exceeding that of plastic beads for any value of $\omega$. According to Eq. (9), this means that the interstices between the particles are smaller in the case of glass beads.

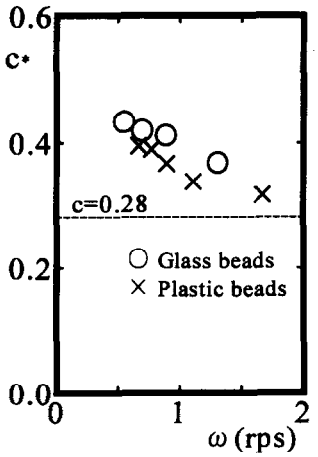


**Fig.6.** Relationship of rotation speed of rolling mill, $\omega$ and mean sediment concentration, $c_*$

**Figure 7** shows the distributions of $p_f/\rho$ measured through the pitot tube. They exhibit the following characteristics:

(a) The pore water pressure within the mixture invariantly exceeds the hydrostatic pressure.

(b) The $p_f$ distribution exhibits a nearly linear trend, thus supporting the assumption of a constant value of $c$.

(c) A higher $p_f$ is obtained increasing the rotation speed $\omega$;

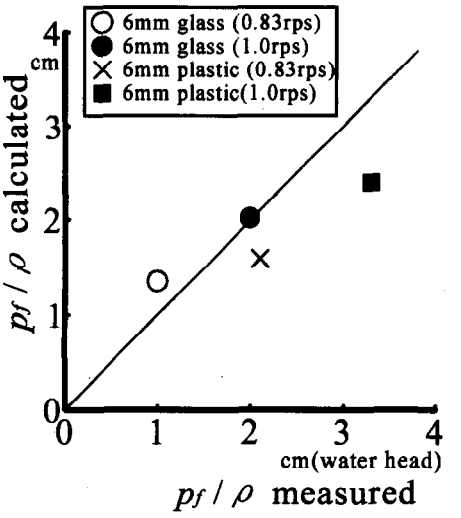


**Fig.8.** Comparison between the measured and calculated values of $p_f/\rho$

(d) for a given value of $\omega$, $p_f$ is higher in the mixture of plastic beads than in the mixture of glass beads, although the specific gravity of the glass beads is greater.

The higher values of $p_f$ associated with the plastic bead mixture are explained by the longer mixing length which, as previously discussed, characterizes the plastic bead mixture.

Finally, we calculated the values for $p_f$ by substituting the experimental values of the various parameters in Eq. (11): the comparison between estimated and measured values of $p_f$ is shown in **Fig.8**. The reasonably good agreement between observed and calculated $p_f$ supports the assumption for $\tau_f$ made by Egashira *et al.* (1989).

Future studies are still needed to examine the relationship between $p_f$ and $\tau_f$ under a wider range of experimental conditions.

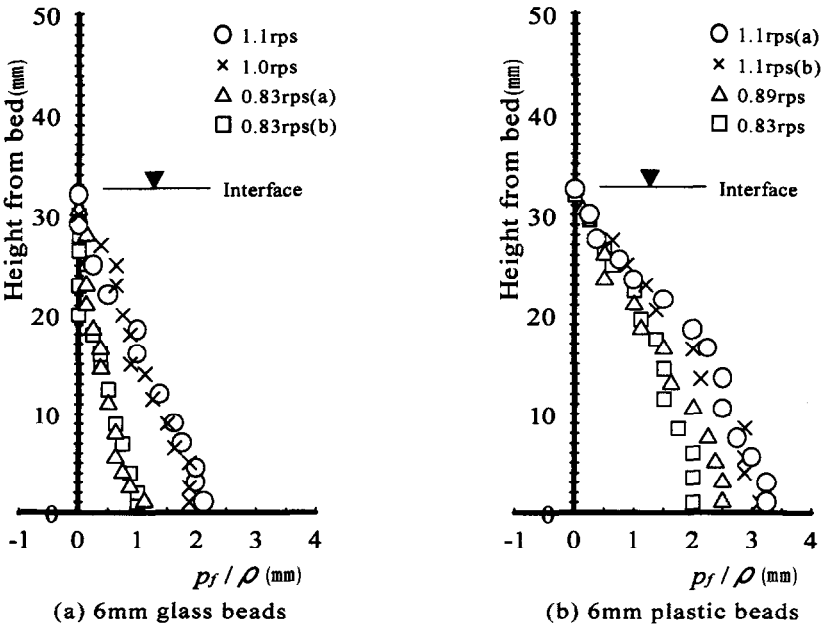


**Fig.7.** Measured vertical distribution of $p_f/\rho$

## References.


Bagnold, R. A. (1954) Experiments in a gravity-free dispersion of large solid spheres in a Newtonian fluid under shear., Proc. Royal Soc. London, *Ser A, 225*, 49-63.

Egashira, S., Ashida, K., Yajima, H., and Takahama J.(1989) Constitutive Equation of Debris Flow., Ann. Disaster Prevention Research Institute, Kyoto Univ., *No.32, B-2*, 487-501 (in Japanese).

Egashira, S. and Ashida, K. (1992) Unified View of the Mechanics of Debris Flow and Bed-Load., Advances in Micromechanics of Granular Materials, Elsevier, 391-400.

Egashira, S., Miyamoto, K., and Itoh T. (1997) Constitutive equations of debris flow and their applicability. *Proc. 1st Int. Conf., Debris-Flow Hazards Mitigation*, ASCE, 340-349.

Hotta, N., Miyamoto, K., Suzuki, M., and Ohta, T. (1998) Pore-water pressure distribution of solid-water phase flow in a rolling mill., Journal of the Japan Society of Erosion Control Engineering, *50(6)*, 11-16 (in Japanese).

Itoh, T. and Egashira, S. (1999) Comparative study of constitutive equations for debris flows. *J. of Hydroscience and Hydraulic Engineering, Vol. 17, No.1*, 59-71.

Krumbein, W. C. (1941) The effects of abrasion on the size, shape and roundness of rock fragments., J. Geology, *49*, 482-520.

Kuenen, P. H. (1956) Experimental abrasion of pebbles 2. Rolling by current., J. Geology, *64*, 336-368.

Miyamoto, K. (1985) Mechanics of Grain Flows in Newtonian Fluid., Ph. D.-thesis presented to Ritsumeikan Univ., (in Japanese).

Takahashi, T. (1980) Debris flow on prismatic open channel. *Proc. ASCE, 106, HY3*, 381-396.